

## HYBRID FLOW CONTROL FOR MICRO AERIAL VEHICLE WITH PORTUBERANCE WING AND MORPHING SURFACE

A. Esmacili, M. Darbandi  
Dept. aerospace engineering  
Sharif University of Technology  
Tehran, Iran

G.E. Schneider  
Dept. mechanical engineering  
University of Waterloo  
Waterloo, Canada

**Abstract**—This study presents new developments required for fixed-wing MAVs, aiming to increase their aerodynamic performance and maneuverability. Since these small vehicles have been restricted by the weight and space requirement to mount batteries inside them, the flight endurance and performance have been sharply decreased. To overcome on the weaknesses, flow control techniques such as passive and active controls would be effective on the small flying vehicles. Recently, a passive flow control solution inspired from the pectoral flippers of humpback whales has been already used which could delay or mitigate out aerodynamic stall. However, an inverse behavior has been found in pre-stall conditions with dropping down the lift coefficients due to the formation of laminar separation bubble (LSB) in the trough section of wing. In the current investigation, in an attempt to retrieve the lift-generation capabilities of the modified wing at pre-stall angles of attack, an active flow control method is designed and numerically simulated, making use of morphing plate specially on the area of the LSB position. The resulting hybrid flow control system has proved its effectiveness, exhibiting complete suppression of the LSB at pre-stall, a delay in the occurrence of stall, and generalized lift enhancements irrespectively of the regime of operation.

**Keywords-component; Hybrid control; Micro air vehicles (MAV); Laminar Separation Bubble; morphing plate.**

### I. INTRODUCTION

Recently, using leading edge tubercles on airfoils, wings, hydrofoils, fans and turbines have seen increased interests of scientists from different areas as a novel passive flow control technique. The original idea was inspired from a humpback whale flipper which is capable of performing acrobatic maneuvers, tight curves, high speed, banked turns as well as loops and rolls [1][2][3]. The morphology and placement of leading edge tubercles reveal that they enhance the lift to control the flow over the whale's flipper, and maintain lift at high angles of attack [4], consequently, delay stall [5]. These interesting abilities have attracted the aerodynamicists' attention to use the same methodology in the real wings, especially in Micro Aerial Vehicles (MAV). Due to the small size and low velocities of

MAVs, they operate in the low Reynolds number regime ( $Re < 200,000$ ), viscous effects are dominant, which degrades lifting surfaces efficiency such as laminar separation, transition and reattachment and unsteady flow effects [6]. Various studies have demonstrated that implementing tubercles could help in reducing the current problems in the low Reynolds number flow region. Initial investigations focused on very specific high-aspect ratio tapered wings as an attempt to mimic a real whale flipper, both from the experimental [5] and computational points of view [7]. Even more recently, Particle Image Velocimetry (PIV) measurements have been carried out as well for different airfoil geometries [8][9], bringing additional insight about the physical mechanisms behind this type of flow control [10]. Parallel to the experimental attempts, numerical predictions of the flow around baseline and modified wings have lately been performed by employing various turbulence models [11][12][13][14][15]. In a nutshell, all of the previous studies indicate that the tubercle leading edge could manipulate the flow and finally delay the stall [16][17][18]. As shown in Fig. 1, a decrease in lift performance is, nevertheless, observed in pre-stall operation. However, these studies also identified the appearance of locally separated flow and forming a LSB on the suction side, even at relatively low incidences (i.e. pre-stall operation), not only as a consequence of the use of rather thick wing sections but namely resulting from the leading-edge modification. Then, the bubble changes the effective form of an airfoil section and subsequently, aerodynamic performance is degraded. Therefore, controlling the bubble would cause accomplished lead to a class of air vehicle aerodynamically very efficient.

Concerning the literature, the effectiveness of plasma actuator for a separated flow, as an active control device, has been demonstrated [19][20]. But a large actuator profile above the surface may inadvertently trip the flow causing premature separation or an early transition to turbulent flow, increasing the skin friction drag, making the plasma actuator ineffective [21] specially in the case of an MAV.

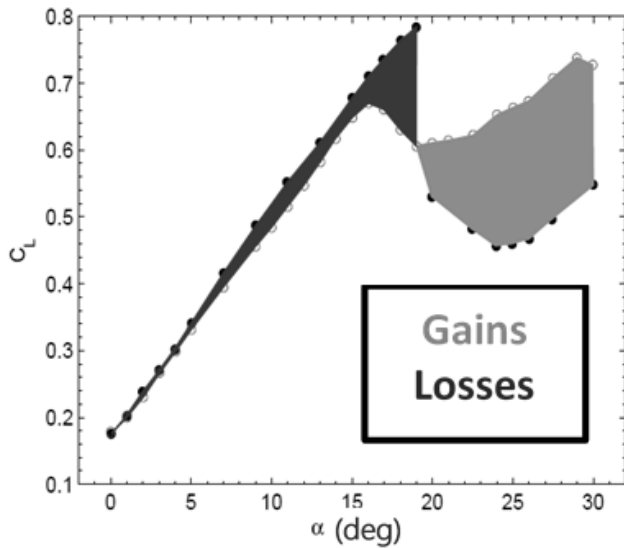


Figure 1. Gains and losses in lift characteristics for a finite-wing with a sinusoidal leading edge (SLE) operating at  $Re = 140,000$ , with respect to the baseline wing. Experimental data from [18].

Another traditional way to control the flow is blowing air jets inside the boundary layer where the flow would like to separate from the surface [22]. Control of flow over a NACA2415 airfoil which experiences an LSB at a transitional Reynolds number of  $2 \times 10^5$  is computationally investigated using blowing or suction [23]. Moreover, an AFC via steady normal blowing has been employed at a Reynolds number of  $6.4 \times 10^4$  on the NACA 643–618 airfoil and the blowing ratio was optimized by maximizing the lift coefficient with minimal power requirement [24]. Furthermore, a tangential blowing has been injected inside the bubble, which was appeared at the trailing edge, by [25]. To have a better efficient of air jets, a pulsating jet has been used to manipulate LSB [26]. However, this blowing actuator needs some equipment such as pump and tubes which increases the weight of MAVs inappropriately. In addition, zero-net-mass-flux injection devices have been recently developed to control the LSB [27], but mass injection into the bubble causes a strong mass imbalance affecting the shear layer entrainment characteristics [28]; consequently, these actuators have been identified as a potential practical means of applying the control strategy outlined in this paper.

In order to overcome the mentioned disadvantages appeared in MAVs application, micro flow control devices consist of morphing plate is being interested whereas a lot of investigations have been carried out on this subject, too. Therefore, a hybrid flow control is numerically investigated to control laminar separation bubble formed at the leading edge of a fixed-wing MAV prototype in the current study. The applied passive method which modifies the leading edge of the wing with a sinusoidal function inspired from nature is proposed to control stall phenomena. However, laminar boundary layer separates at the leading edge and the bubble appears on the pressure surface of the SLE wing at the pre-stall condition which is caused a reduction in the aerodynamic efficiency. Solving this inflection is one of the main objectives of this study and the only way is eliminating or controlling LSBs by the morphing surface as an

effective active control. The actuator surface can deform based on the pressure distribution on the separation area and the airfoil sectional shape is changed correctly.

## II. NUMERICAL METHODOLOGY

### A. Computational Meshes

A C-H-topology was selected to produce the computational meshes around the models. The far field boundary was set at a distance of  $20c$  in upstream and downstream of the wing and  $13c$  in the spanwise directions from the wing tip. In these simulations, a periodicity condition was imposed at the spanwise face boundaries of the computational domain. Finally, as the flow remained incompressible in all studied cases, a simple open boundary condition was used at the outflow section at a distance of  $12c$ , and no-slip conditions were applied to the wall surfaces of the wing. The domain extension was designed so that the inlet and outlet planes did not affect the flow over the wing vicinity.

To produce hexahedral elements in the mesh, the computational domain was split into four volumes. Each volume was meshed individually to have a desired cell density in the region; although it is a time-consuming process to mesh multiple volumes, doing so provided control over the mesh density. The cell quality is also important to ensure a good mesh, which is measured by the parameters equiskew and aspect ratio. The aspect ratio and equiskew of cells are maintained within the range throughout the domain. The leading edge protuberance induces more complexity to the mesh procedure with hexahedral elements near the surface of the wing. To avoid inverted cell volumes and high skewness, the least possible cell distance near the wall is applied while the maximum value of  $Y^+$  was around 1 and the minimum requirement for DES model[29] was satisfied. Concerning computational limits on the size of the grid, different numerical meshes were employed in the analysis of the flow around the wing. Then, the pressure coefficient distribution on the wing surface was compared for all the meshes and that mesh was kept unchanged irrespective of the turbulence model has been applied. As a consequence, the overall amounts of cells was  $1.35 \times 10^7$  for aspect ratio 1.5 (Fig. 2).

### B. Numerical Method

The computational procedure used a SIMPLE (Semi-Implicit Method for Pressure-Linked Equations) pressure-velocity coupling and a second-order accurate spatial discretization for the pressure. The QUICK (Quadratic Upwind Interpolation for Convective Kinematics) scheme was used in the discretization of momentum and turbulence equations.[30] However, the time integration was performed employing a second-order accurate implicit scheme to alleviate numerical stability restrictions. The time step used was  $0.0025$  s in all simulations. The model chord and the freestream velocity were fixed to  $0.232$  m and  $8.815$  m/s, respectively. It corresponds to a Reynolds number  $Re$  of  $140,000$ , within the typical range of operation of MAVs. In a significant number of cases, the simulations had to be carried out for longer than  $40$  s in order to reach a stable (unsteady) behavior unaffected by initial

transients. In this study, the aforementioned steps of the solution are performed by ANSYS Fluent version 15 solver, which computes the fluid field. Hence, the model equation and the interactions between the flow and structure are carried out via a user-defined-function (UDF) within Fluent.

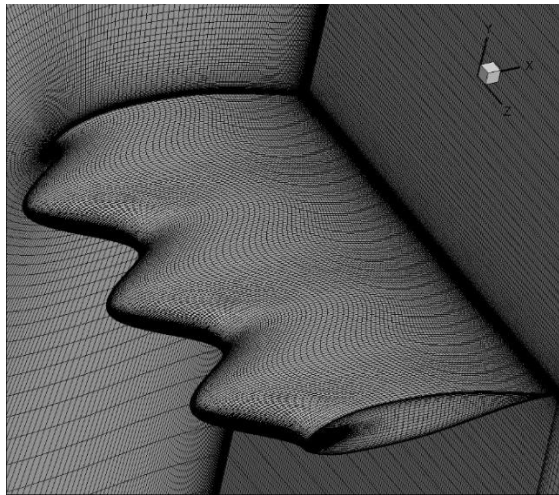


Figure 2. Illustration of the computational mesh for tubercle wing AR=1.5

### C. Turbulence Modeling

Taking into account the geometry of the models and the selected Reynolds number, LES, and DNS (Direct Numerical Simulation) were deemed too computationally expensive and, therefore, were discarded. It was chosen DDES over unsteady RANS with different shielding function to find the best model for various conditions. DDES approach is known to perform better when massive separations occur,[31] which is expected to arise for the models operating at high angles of attack. Since the original Detached Eddy Simulation (DES) demonstrated an artificial separation which depends on the grid spacing and not the flow physics,[32] the switch zone from RANS to LES model could be protected by shielding functions. The resulting formulation was named Delayed option.[33] The mentioned method is a hybrid between LES and RANS, as it uses the latter to resolve the boundary layer. For this purpose, the selected turbulence model was the SST  $k-\omega$ . [32] The reason is twofold: firstly, because this modeling procedure can be coupled with transition prediction via a transport equation for intermittency; secondly, because of the superior performance of this model at reducing the mesh influence of the DDES limiter in the RANS boundary layer [31].

### D. Validations

To check the degree of accuracy in the present CFD data, the aerodynamic coefficients are compared with the experimental data obtained by this study. The SLE wing model with AR=1.5 is chosen, and its lift (CL) and drag (CD) coefficients are compared with the experimental ones, as shown in Fig. 3. The comparison demonstrates that the numerical

results are in excellent agreement with those of experimental values. Usually, the CL values are easy to predict because they are mainly due to the pressure difference between the upper and lower surfaces of the wing. Typically, the CD values show poor agreement in turbulent flows since they are primarily caused by skin friction especially in high angle of attack. However, the values shown here have a good deal.

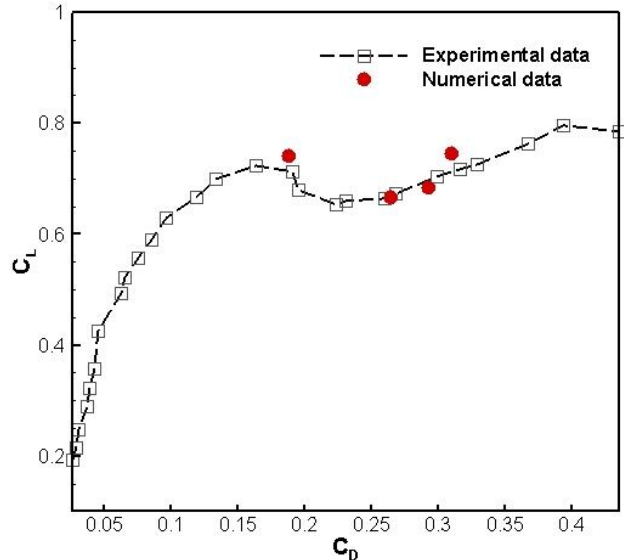


Figure 3. Polar comparison of lift and drag coefficients of modified wing between present numerical and experimental outputs [34] at AR=1.5.

### E. Morphing geometry and model equation

More recently, the development of new actuation devices and material systems has enabled novel approaches to flow control still to be explored. These systems deform the surface of the airfoil to introduce disturbances into the flow. Additionally, they would no longer be a source of additional drag in the switched-off condition. Therefore, a thin, flexible macro-fiber composite (MFC) actuator is considered here to morph the surface of an airfoil at such low Reynolds number flow. When embedded in a surface or attached to flexible structures, such actuators provide a distributed force with little power consumption. These actuators are also very light and easy to integrate to the surface of an airfoil, thus maximizing their possible aerodynamic gains. MFC actuators consist of three main components: 1) a sheet of aligned piezoceramic fibers; 2) a pair of thin polymer films etched with a conductive electrode pattern; and 3) an adhesive matrix material. It is also noteworthy that these systems only provide very small deformation amplitudes, and they are very susceptible to the fluid loading and have a constant production of maximum deflection. In case of small deflections, the force and the corresponding shape of the beam can be approximated by using a Rayleigh-Ritz weighted residual method [35]. The force induced by the fluid flow is obtained from the pressure distribution and wall viscous shear stress by integration over the surface of the morphing surface. The spatially distributed fluid force in each mesh cell is projected onto the mass normalized eigenfunctions, as follows:

$$f(t) = \int_{x=0}^L (f_p(x,t) + f_v(x,t)) \phi_r(x) dx \quad (1)$$

where  $f_p(x,t)$  and  $f_v(x,t)$  are the net pressure and viscous forces acting on the mentioned surface. Also  $\phi_r(x)$  is the weighting function for the first-mode shape assumed to be:

$$\phi_r(x) = 1 - \cos\left(\frac{2\pi x}{L}\right) \quad (2)$$

In each time step, the fluid-induced force  $f$  is assumed constant and used in the solution of the structure equation. The force is applied to the center of beam and, as shown in Fig. 4, the deflection of each point ( $y$ ) can be obtained by the following equation:

$$y(x) = \frac{fx}{48EI}(3L^2 - 4x^2) \quad (3)$$

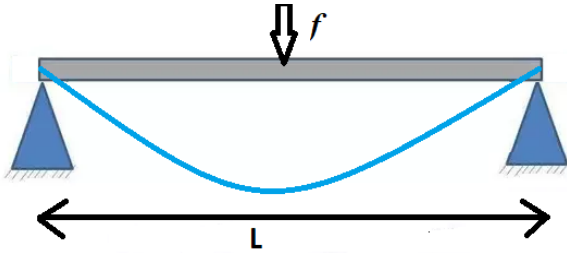


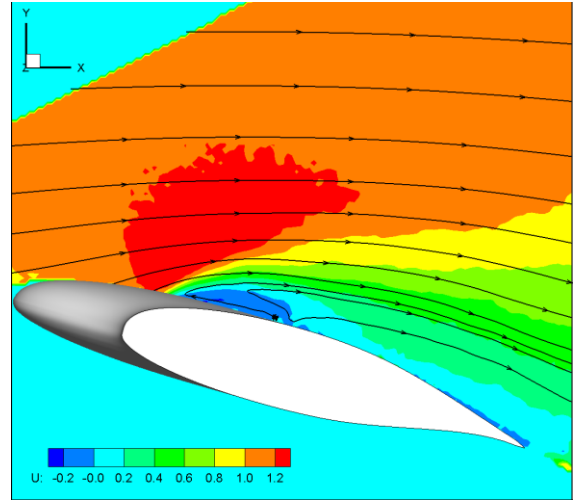
Figure 4. Hinted end beam used as a morphing geometry model.

### III. RESULTS AND DISCUSSIONS

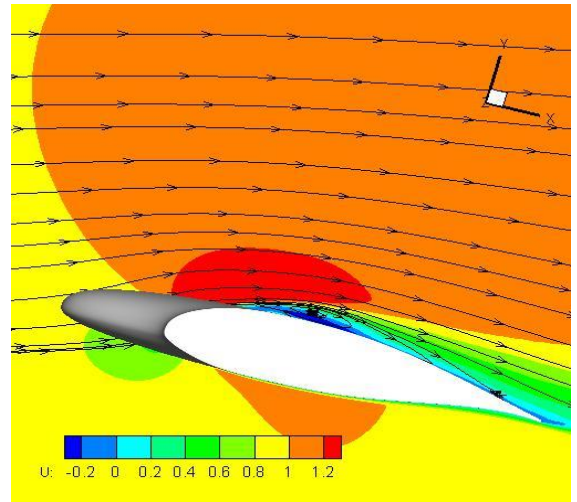
#### A. Effect of Leading Edge Modification

As Fig. 1 illustrated, sinusoidal leading edge modification has a positive effect in post-stall angles when compared to the baseline wing; but, the wing efficiency was damaged specially in pre-stall condition. Since a laminar separation bubble (LSB) was appeared on the suction side of SLE wing model at the trough cross-section based on Stereo PIV images in [36][34], the numerical simulation is carried out in this study to obtain more details of flow field. As noted in previous study [37], RANS models have poor performance in the separated flow regions and otherwise, a high mesh resolution in wall-bounded flow would be required in resolved turbulence models such as LES which increases the computational costs. Then, a hybrid RANS/LES modeling is an attractive alternative approach to combine the advantages of both RANS and LES models. Therefore, IDDES model was introduced which combines WMLES and DDES models and the laminar separation bubble could correctly forecast by this approach, simulate a tiny reattached bubble and without any momentous trailing edge separation. To have a better comparison, the streamline contour plots of normalized x-velocity at the trough section of SLE wing were compared to the experimental one [34] at AOA=15°. Apparently, in Fig. 5, the IDDES model is able to generate a turbulent boundary layer over the upper surface, leading to laminar separation at the leading edge. Furthermore, this model operated very well at the trailing edge, thus seemingly producing results that are closer to those obtained with Stereo PIV. In this

figure, the ability of correctly reproducing an experimental operating condition characterized by capturing the laminar separation bubble on the wing can be seen as an adequate quality of the model and the same approach would be therefore used in the entire following cases.



(a)



(b)

Figure 5. Normalized time-averaged x-velocity obtained by stereo PIV measurement [34] and IDDES model around the tubercle wing at AOA=15 deg.

#### B. Active Flow Control System

The separated bubble alters the effective shape of SLE wing, and as a result of this, the accelerated flow area in the suction side would be smaller comparing with traditional wing model which influences on the aerodynamic coefficients. Honestly, the flow in the mentioned low Reynolds number is laminar and is dominated by viscous effects. Due to the low momentum, the flow could not move to downstream, and it tends to separate before being turbulent. After laminar flow separation, the flow structure becomes sharply irregular, and under this circumstance, a transition phenomenon from laminar to

turbulent occurs. Since the flow in the free stream is more energetic, the turbulent mixing process redeploys high-momentum fluid to the separated layer and then confronts to the adverse pressure gradient, and finally, the flow is squeezed to reattach. Moreover, some parameters such as Reynolds number, incidence angle, surface roughness, wing shape and free stream turbulence play a significant role on the dynamic of LSB; however, the balance between two competitors, high-momentum flow and adverse pressure gradient, defines the length of bubble. Therefore, morphing surface can modify the wing shape and depending on the pressure distribution on the wing surface, it is deformed and the separation bubble did not form as shown in Fig. 6. On the other word, LSB generates a low pressure area on the surface and the morphing surface deforms positively.

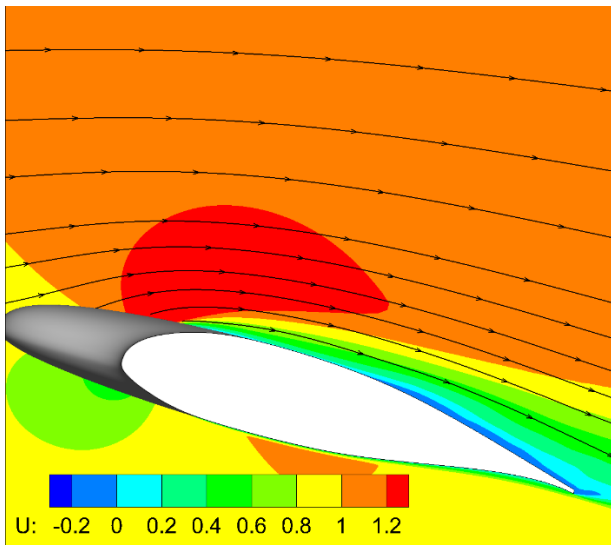


Figure 6. Normalized time-averaged x-velocity obtained by IDDES model around the tubercle wing with morphing actuator.

## CONCLUSION

Numerical investigation of the flow over the finite tubercle wing in  $AR=1.5$  was conducted at  $Re=140,000$ . Initially, the effect of leading edge shape modification of wing as a passive stall control was studied and the most important conclusion from passive control is that this modification has provided a better performance in post-stall condition because of appearing the superior streamwise vortices generated by the tubercles at the leading edge and as a result of this, the intensified momentum transport at peak and trough sections intend to maintain lift and preventing stall. In contrast, this passive control did not operate positively in pre-stall circumstances and the lift coefficient has a drop compared with the baseline wing. Comparison of the computed results with the experimental data on the SLE wing has also carried out which has effectively demonstrated a presence of laminar separation bubble as the main reason of this differences.

To solve the aforementioned discrepancies, an active flow control has been designed in this investigation, focusing on the effect of morphing surfaces on the topology of the flow and

laminar separation bubble at low Reynolds number. Therefore, the actuator was established in the trough section of wing where the bubbles appear. Finally, the results demonstrated that the morphing surfaces had a substantial impact in pre-stall regimes such that the lift coefficient revived in these incidence angles.

## REFERENCES

- [1] F. Fish and J. Battle, "Hydrodynamic design of the humpback whale flipper," *J. Morphol.*, vol. 225, no. 1, pp. 51–60, 1995.
- [2] C. Canning et al., "Population-level lateralized feeding behaviour in North Atlantic humpback whales, *Megaptera novaeangliae*," *Anim. Behav.*, vol. 82, no. 4, pp. 901–909, 2011.
- [3] F. E. Fish, L. E. Howle, and M. M. Murray, "Hydrodynamic flow control in marine mammals," *Integr. Comp. Biol.*, vol. 48, no. 6, pp. 788–800, Dec. 2008.
- [4] D. Miklosovic, M. Murray, and L. Howle, "Experimental evaluation of sinusoidal leading edges," *J. Aircr.*, vol. 44, no. 4, pp. 1404–1408, 2007.
- [5] D. S. Miklosovic, M. M. Murray, L. E. Howle, and F. E. Fish, "Leading-edge tubercles delay stall on humpback whale (*Megaptera novaeangliae*) flippers," *Phys. Fluids*, vol. 16, no. 5, p. L39, 2004.
- [6] M. Gad-el-Hak, *Flow control : passive, active, and reactive flow management*. Cambridge University Press, 2006.
- [7] H. Carreira Pedro and M. Kobayashi, "Numerical study of stall delay on humpback whale flippers," in 46th AIAA Aerospace Sciences Meeting and Exhibit, 2008.
- [8] M. Zhang, G. Wang, and J. Xu, "Aerodynamic control of low-Reynolds-number airfoil with leading-edge protuberances," *AIAA J.*, vol. 51, no. 8, pp. 1960–1971, 2013.
- [9] M. Zhang, G. Wang, and J. Xu, "Effect of humpback whale-like leading-edge protuberances on the low Reynolds number airfoil aerodynamics," *Fluid-Structure-Sound Interact.*, pp. 107–113, 2014.
- [10] N. Rostamzadeh and K. Hansen, "The formation mechanism and impact of streamwise vortices on NACA 0021 airfoil's performance with undulating leading edge modification," *Phys. Fluids*, vol. 26, no. 10, p. 107101, 2014.
- [11] P. Watts and F. Fish, "The influence of passive, leading edge tubercles on wing performance," in Proc. Twelfth Intl. Symp. Unmanned Untethered, 2001.
- [12] A. Dropkin, D. Custodio, C. W. Henocho, and H. Johari, "Computation of flow field around an airfoil with leading-edge protuberances," *J. Aircr.*, vol. 49, no. 5, pp. 1345–1355, Sep. 2012.
- [13] J. Favier, A. Pinelli, and U. Piomelli, "Control of the separated flow around an airfoil using a wavy leading edge inspired by humpback whale flippers," *Comptes Rendus Mécanique*, vol. 340, no. 1, pp. 107–114, 2012.
- [14] H. Arai, D. Yasuaki, N. Takuji, and M. Hidemi, "Numerical simulation around rectangular wings with wavy leading edge," *J. Japan Soc. Nav. Archit. Ocean Eng.*, vol. 12, pp. 33–41, 2010.
- [15] A. Malipeddi, N. Mahmoudnejad, and K. Hoffmann, "Numerical analysis of effects of leading-edge protuberances on aircraft wing performance," *J. Aircr.*, vol. 49, no. 5, pp. 1336–1344, 2012.
- [16] H. Johari, C. W. Henocho, D. Custodio, and A. Levshin, "Effects of leading-edge protuberances on airfoil performance," *AIAA Journal*, vol. 45, no. 11, pp. 2634–2642, 2007.
- [17] D. Custodio, C. W. Henocho, and H. Johari, "Aerodynamic characteristics of finite span wings with leading-edge protuberances," *AIAA J.*, vol. 53, no. 7, pp. 1878–1893, Jul. 2015.
- [18] J. L. E. Guerreiro and J. M. M. Sousa, "Low-Reynolds-number effects in passive stall control using sinusoidal leading edges," *AIAA J.*, vol. 50, no. 2, pp. 461–469, Feb. 2012.
- [19] M. Sato et al., "Mechanisms for laminar separated-flow control using dielectric-barrier-discharge plasma actuator at low Reynolds number," *Phys. Fluids*, vol. 27, no. 11, p. 117101, Nov. 2015.
- [20] M. G. De Giorgi, A. Ficarella, F. Marra, and E. Pescini, "Micro DBD plasma actuators for flow separation control on a low pressure turbine at high altitude flight operating conditions of aircraft engines," *Appl. Therm. Eng.*, vol. 114, pp. 511–522, 2017.

- [21] T. West and S. Hosder, "Numerical investigation of plasma actuator configurations for flow separation control at multiple angles of attack," 6th AIAA Flow Control Conf., 2012.
- [22] A. Farhadi, E. G. Rad, and H. Emdad, "Aerodynamic multi-parameter optimization of NACA0012 airfoil using suction/blowing jet technique," Arab. J. Sci. Eng., pp. 1–9, Jul. 2016.
- [23] M. Genç and Ü. Kaynak, "Control of Flow Separation and Transition Point over an Aerofoil at Low Re Number using Simultaneous Blowing and Suction," in 19th AIAA Computational Fluid Dynamics, 2009.
- [24] N. O. Packard, M. P. Thake, C. H. Bonilla, K. Gompertz, and J. P. Bons, "Active control of flow separation on a laminar airfoil," AIAA J., vol. 51, no. 5, pp. 1032–1041, May 2013.
- [25] P. Viswanath and K. Madhavan, "Control of trailing-edge separation by tangential blowing inside the bubble," Aeronaut. J., vol. 108, no. 6, pp. 419–425, 2004.
- [26] Y. H. Choi and H. B. Kim, "Pulsating jet control for manipulating the separation bubble behind the fence," J. Vis., vol. 13, no. 3, pp. 221–228, Aug. 2010.
- [27] O. Marxen, R. B. Kotapati, R. Mittal, and T. Zaki, "Stability analysis of separated flows subject to control by zero-net-mass-flux jet," Phys. Fluids, vol. 27, no. 2, p. 024107, Feb. 2015.
- [28] M. Jahanmiri, Laminar Separation Bubble An overview on research works on characteristics, dynamics, and control of LSBs. LAP LAMBERT Academic Publishing, 2013.
- [29] P. R. Spalart and C. Streett, "Young-person's guide to detached-eddy simulation grids," 2001.
- [30] J. Pereira and J. M. M. Sousa, "Finite volume calculations of self-sustained oscillations in a grooved channel," J. Comput. Phys., vol. 106, no. 1, pp. 19–29, 1993.
- [31] M. Ilak, P. Schlatter, and S. Bagheri, "Bifurcation and stability analysis of a jet in cross-flow: onset of global instability at a low velocity ratio," J. Fluid, vol. 696, pp. 94–121, 2012.
- [32] F. Menter, M. Kuntz, and R. Langtry, "Ten years of industrial experience with the SST turbulence model," Turbul. heat mass Transf., 2003.
- [33] P. R. Spalart, S. Deck, M. L. Shur, K. D. Squires, M. K. Strelets, and A. Travin, "A new version of detached-eddy simulation, resistant to ambiguous grid densities," Theor. Comput. Fluid Dyn., vol. 20, no. 3, pp. 181–195, Jul. 2006.
- [34] A. Esmaili, H. E. C. Delgado, and J. M. M. Sousa, "Numerical simulations of low-Reynolds-number flow past finite wings with leading-edge protuberances," J. Aircr., vol. 55, no. 1, pp. 226–238, Oct. 2018.
- [35] H. D. Akaydin, N. Elvin, and Y. Andreopoulos, "Energy harvesting from highly unsteady fluid flows using piezoelectric materials," J. Intell. Mater. Syst. Struct., vol. 21, no. 13, pp. 1263–1278, Sep. 2010.
- [36] H. Delgado, A. Esmaili, and J. M. M. Sousa, "Stereo PIV measurements of low-aspect-ratio low-Reynolds-number wings with sinusoidal leading edges for improved computational modeling," in Proc 52st AIAA Aerospace Sciences Meeting, 2014.
- [37] A. Esmaili and J. M. M. Sousa, "Influence of wing aspect ratio on passive stall control at low Reynolds number using sinusoidal leading edges," in 29th Congress of the International Council of the Aeronautical Sciences, 2014.